that has thus far been restricted to a purely theoretical framework.

REFERENCES AND NOTES

1. K. S. Novoselov *et al.*, *Science* **306**, 666–669 (2004).
2. P. O. Lehtinen, A. S. Foster, Y. Ma, A. V. Krasheninnikov, R. M. Nieminen, *Phys. Rev. Lett.* **93**, 187202 (2004).
3. V. M. Pereira, F. Guinea, J. M. Lopes dos Santos, N. M. R. Peres, A. H. Castro Neto, *Phys. Rev. Lett.* **96**, 036801 (2006).
4. O. V. Yazyev, L. Helm, *Phys. Rev. B* **75**, 125408 (2007).
5. O. V. Yazyev, *Rep. Prog. Phys.* **73**, 056501 (2010).
6. E. J. G. Santos, A. Ayuela, D. Sanchez-Portal, *New J. Phys.* **14**, 043022 (2012).
7. E. H. Lieb, *Phys. Rev. Lett.* **62**, 1201–1204 (1989).
8. J. Fernández-Rossier, J. J. Palacios, *Phys. Rev. Lett.* **99**, 177204 (2007).
9. J. J. Palacios, J. Fernández-Rossier, L. Brey, *Phys. Rev. B* **77**, 195428 (2008).
10. M. Fujita, K. Wakabayashi, K. Nakada, K. Kusakabe, *J. Phys. Soc. Jpn.* **65**, 1920–1923 (1996).
11. C. G. Tao *et al.*, *Nat. Phys.* **7**, 616–620 (2011).
12. M. M. Ugeda, I. Brihuega, F. Guinea, J. M. Gómez-Rodríguez, *Phys. Rev. Lett.* **104**, 096804 (2010).
13. R. R. Nair *et al.*, *Nat. Phys.* **8**, 199–202 (2012).
14. K. M. McCreary, A. G. Swartz, W. Han, J. Fabian, R. K. Kawakami, *Phys. Rev. Lett.* **109**, 186604 (2012).
15. R. R. Nair *et al.*, *Nat. Commun.* **4**, 2010 (2013).
16. J. Balakrishnan, G. Kok Wai Koon, M. Jaiswal, A. H. Castro Neto, B. Özyilmaz, *Nat. Phys.* **9**, 284–287 (2013).
17. L. Jeloaica, V. Sidis, *Chem. Phys. Lett.* **300**, 157–162 (1999).
18. X. W. Sha, B. Jackson, *Surf. Sci.* **496**, 318–330 (2002).
19. D. W. Boukhvalov, M. I. Katsnelson, A. I. Lichtenstein, *Phys. Rev. B* **77**, 035427 (2008).
20. D. Soriano *et al.*, *Phys. Rev. Lett.* **107**, 016602 (2011).
21. F. Varchon, P. Mallet, L. Magaud, J. Y. Veuillen, *Phys. Rev. B* **77**, 165415 (2008).
22. M. Sprinkle *et al.*, *Phys. Rev. Lett.* **103**, 226803 (2009).
23. G. H. Li *et al.*, *Nat. Phys.* **6**, 109–113 (2010).
24. G. Trambly de Laissardière, D. Mayou, L. Magaud, *Nano Lett.* **10**, 804–808 (2010).
25. H. A. Mizes, J. S. Foster, *Science* **244**, 559–562 (1989).
26. P. Ruffieux, O. Groning, P. Schwaller, L. Schlapbach, P. Groning, *Phys. Rev. Lett.* **84**, 4910–4913 (2000).
27. Materials and methods are available as supplementary materials on *Science* Online.
28. P. W. Anderson, *Phys. Rev.* **124**, 41–53 (1961).
29. B. Uchoa, V. N. Kotov, N. M. R. Peres, A. H. Castro Neto, *Phys. Rev. Lett.* **101**, 026805 (2008).
30. L. Hornekær *et al.*, *Phys. Rev. Lett.* **97**, 186102 (2006).
31. Z. Sljivančanin *et al.*, *J. Chem. Phys.* **131**, 084706 (2009).
32. R. Balog *et al.*, *J. Am. Chem. Soc.* **131**, 8744–8745 (2009).
33. M. Eigler, E. K. Schweizer, *Nature* **344**, 524–526 (1990).
34. T. C. Shen *et al.*, *Science* **268**, 1590–1592 (1995).
35. A. A. Khajetoorians *et al.*, *Science* **339**, 55–59 (2013).
36. I. Horcas *et al.*, *Rev. Sci. Instrum.* **78**, 013705 (2007).

QUANTUM OPTICS

Bell correlations in a Bose-Einstein condensate

Roman Schmied,[1]* Jean-Daniel Bancal,[2,4]* Baptiste Allard,[1]* Matteo Fadel,[1] Valerio Scarani,[2,3] Philipp Treutlein,[1]† Nicolas Sangouard[4]†

Characterizing many-body systems through the quantum correlations between their constituent particles is a major goal of quantum physics. Although entanglement is routinely observed in many systems, we report here the detection of stronger correlations—Bell correlations—between the spins of about 480 atoms in a Bose-Einstein condensate. We derive a Bell correlation witness from a many-particle Bell inequality involving only one- and two-body correlation functions. Our measurement on a spin-squeezed state exceeds the threshold for Bell correlations by 3.8 standard deviations. Our work shows that the strongest possible nonclassical correlations are experimentally accessible in many-body systems and that they can be revealed by collective measurements.

Parts of a composite quantum system can share correlations that are stronger than any classical theory allows (*1*). These so-called Bell correlations represent the most profound departure of quantum from classical physics and can be confirmed experimentally by showing that a Bell inequality is violated by the system. The existence of Bell correlations at spacelike separations refutes local causality (*2*); thus, Bell correlations are also called nonlocal correlations. Moreover, they are a key resource for quantum technologies such as quantum key distribution and certified randomness generation (*3*). Bell correlations have so far been detected between up to 14 ions (*4*), four photons (*5*, *6*), two neutral atoms (*7*), two solid-state spin qubits (*8*), and two Josephson phase qubits (*9*). Even though multipartite Bell inequalities are known (*1*, *10*–*12*), the detection of Bell correlations in larger systems is challenging.

A central challenge in quantum many-body physics is to connect the global properties of a system to the underlying quantum correlations between the constituent particles (*13*, *14*). For example, recent experiments in quantum metrology have shown that spin-squeezed states of atomic ensembles can enhance the precision of interferometric measurements beyond classical limits (*15*–*18*). This enhancement requires entanglement between atoms in the ensemble, which can be revealed by measuring an entanglement witness that involves only collective measurements on the entire system (*15*, *19*–*22*). The role of Bell correlations in many-body systems, on the other hand, is largely unknown.

[1]Quantum Atom Optics Laboratory, Department of Physics, University of Basel, Klingelbergstrasse 82, 4056 Basel, Switzerland. [2]Centre for Quantum Technologies, National University of Singapore, 3 Science Drive 2, Singapore 117543. [3]Department of Physics, National University of Singapore, 2 Science Drive 3, Singapore 117542. [4]Quantum Optics Theory Group, Department of Physics, University of Basel, Klingelbergstrasse 82, 4056 Basel, Switzerland.
*These authors contributed equally to this work. †Corresponding author. Email: philipp.treutlein@unibas.ch (P.T.), nicolas.sangouard@unibas.ch (N.S.)

Whereas all Bell-correlated states are entangled, the converse is not true (*1*). In recent theoretical work, a family of Bell inequalities was derived that are symmetric under particle exchange and involve only first- and second-order correlation functions (*23*). It was suggested that this could enable the detection of Bell correlations by collective measurements on spin ensembles. Acting on this proposal, we derive a collective witness observable that is tailored to detect Bell correlations in spin-squeezed states of atomic ensembles. We report a measurement of this witness on 480 ultracold rubidium atoms, revealing Bell correlations in a many-body system.

We derive our Bell correlation witness in the context of a Bell test where N observers (indexed by $i = 1...N$) each repeatedly perform one of two possible local measurements $\mathcal{M}_0^{(i)}$ or $\mathcal{M}_1^{(i)}$ on their part of a composite system and observe one of two possible outcomes $a_i = \pm 1$. For example, the system could be an ensemble of atomic spins where each observer is associated with one atom and the measurements correspond to spin projections along different axes. When all observers choose to measure $\mathcal{M}_0$, one determines experimentally the sum of their average outcomes $\mathcal{S}_0 = \sum_{i=1}^N \langle \mathcal{M}_0^{(i)} \rangle$ and correlations $\mathcal{S}_{00} = \sum_{i,j=1(i \neq j)}^N \langle \mathcal{M}_0^{(i)} \mathcal{M}_0^{(j)} \rangle$ [see section 1 of the supplementary materials (*24*) for a definition in terms of measured frequencies]. Similarly, $\mathcal{S}_{11} = \sum_{i,j=1(i \neq j)}^N \langle \mathcal{M}_1^{(i)} \mathcal{M}_1^{(j)} \rangle$ is determined when all observers choose $\mathcal{M}_1$. A more complex correlation $\mathcal{S}_{01} = \sum_{i,j=1(i \neq j)}^N \langle \mathcal{M}_0^{(i)} \mathcal{M}_1^{(j)} \rangle$ is quantified by letting all pairs of observers choose opposite measurements, which requires repeated observations of identically prepared states of the system because some of these measurements are mutually exclusive. In (*23*), a Bell inequality was derived that contains only these symmetric one- and two-body correlators.

$$2\mathcal{S}_0 + \frac{1}{2}\mathcal{S}_{00} + \mathcal{S}_{01} + \frac{1}{2}\mathcal{S}_{11} + 2N \geq 0 \quad (1)$$

If an experiment violates this inequality, the conditional probabilities $P(a_1, ..., a_N | x_1, ..., x_N)$

to obtain measurement results $a_1, ..., a_N$ for given measurement settings $x_1, ..., x_N$ (with $x_i \in \{0,1\}$) cannot be explained by preestablished agreements; i.e., $P(a_1, ..., a_N | x_1, ..., x_N) \neq \int d\lambda \, P(\lambda) \, P(a_1 | x_1, \lambda) \cdots P(a_N | x_N, \lambda)$, where $P(\lambda)$ is the probability of using agreement λ. In this case, we say that the system is Bell-correlated. For illustration, consider again the situation where each observer performs measurements on the spin of an atom in a large ensemble. If the system is Bell-correlated, appropriate measurements on the atomic spins show statistics that cannot be explained by a recipe that determines the measurement results for each atom independently of the measurement results and settings of the other atoms.

The form of $\mathcal{S}_{01}$ demands that we can set the measurement type of each observer individually. Testing the Bell inequality in Eq. 1 thus requires more than collective measurements,

which are sometimes the only available option in many-body systems. A way around this requirement is to replace the Bell inequality, which guarantees both that the state is Bell correlated and that appropriate measurements were actually performed, by a witness inequality that assumes a quantum-mechanical description and correct experimental calibration of the measurements. A similar approach has been successfully employed to detect entanglement with collective measurements only (15, 19–22, 25). We associate each observer i with a spin 1/2 (in our experiment, a pseudospin representing two energy levels of an atom). The measurements are spin projections $\mathcal{M}_d^{(i)} = 2\hat{s}^{(i)} \cdot d$ along an axis d, where $2\hat{s}^{(i)} = \{\hat{\sigma}_x^{(i)}, \hat{\sigma}_y^{(i)}, \hat{\sigma}_z^{(i)}\}$ is the Pauli vector. All other energy levels of the atoms, as well as further degrees of freedom (e.g., atomic motion), are irrelevant for the measurements. We define the total spin observable $\hat{S}_d = d \cdot \sum_{i=1}^{N} \hat{s}^{(i)}$ in the

direction d, which can be probed by collective measurements on the entire system. For two unit vectors a and n, we now consider the observable

$$\hat{W} = -\left| \frac{\hat{S}_n}{N/2} \right| + (a \cdot n)^2 \frac{\hat{S}_a^2}{N/4} + 1 - (a \cdot n)^2 \quad (2)$$

defined in terms of total-spin observables only. Setting $\mathcal{M}_n^{(i)} = \mathcal{M}_0^{(i)}$ and $\mathcal{M}_m^{(i)} = \mathcal{M}_1^{(i)}$ with $m = 2(a \cdot n)a - n$, the expectation value of $\hat{W}$ can be reexpressed in terms of one- and two-body correlations functions using $\langle \hat{S}_n \rangle = \mathcal{S}_0/2$ and $16(a \cdot n)^2 \langle \hat{S}_a^2 \rangle = \mathcal{S}_{00} + 2\mathcal{S}_{01} + \mathcal{S}_{11} + 4N(a \cdot n)^2$; see section 1 of (24). The Bell inequality in Eq. 1 then guarantees that $\langle \hat{W} \rangle \geq 0$ whenever the state of the system is not Bell-correlated. By construction, this Bell correlation witness $\hat{W}$ only involves first and second moments of collective spin measurements along two directions a and n, making it well suited for experiments on many-body
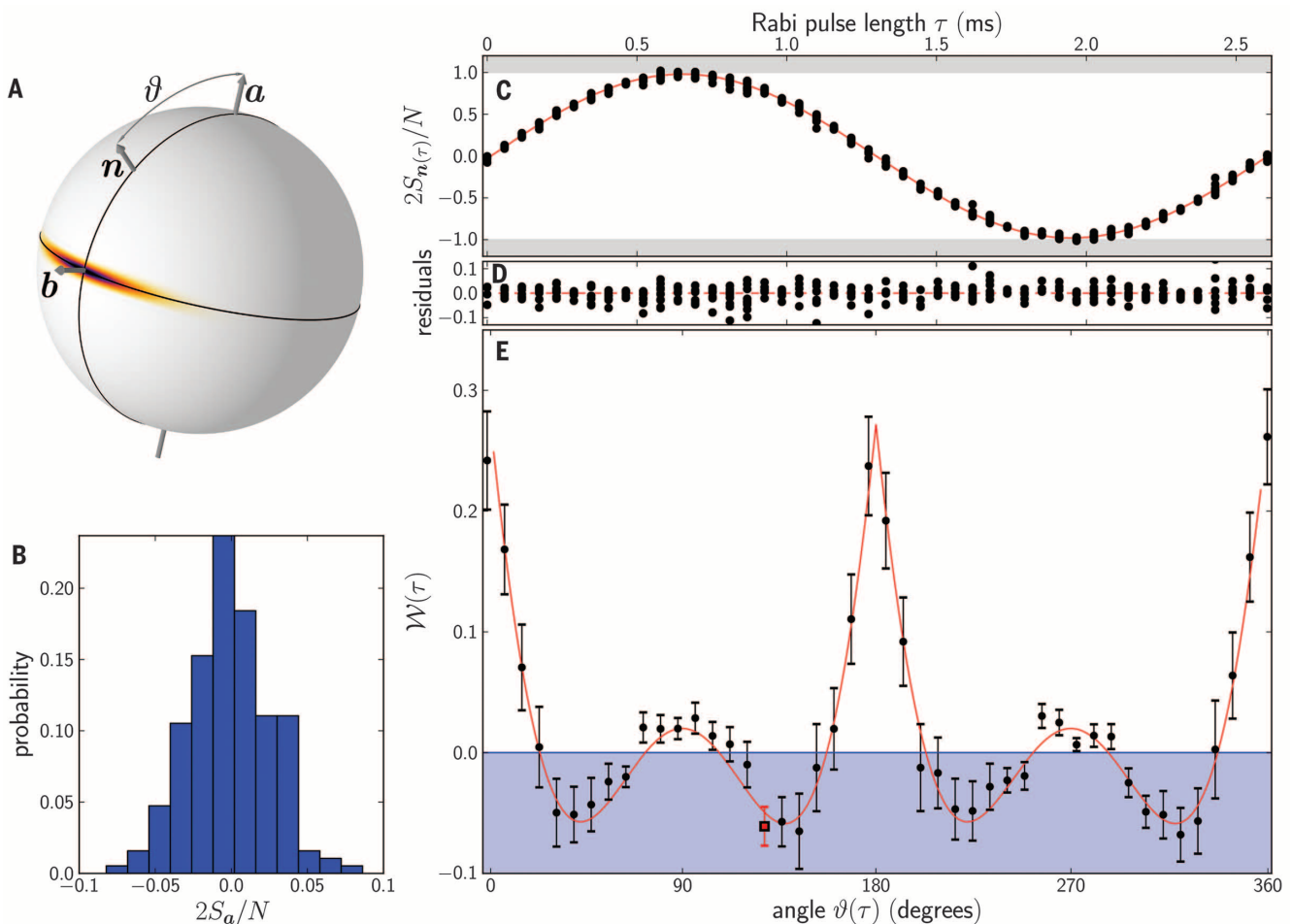

Fig. 1. Observation of Bell correlations in a BEC with the inequality in Eq. 3. (**A**) Illustration of the spin-squeezed state [Wigner function (32)] and the axes used in the measurement of the Bell correlation witness $\mathcal{W}$. The vector n lies in the plane spanned by the squeezing axis a and the state's center b. The squeezing and antisqueezing planes are indicated with thin black lines. (**B**) Histogram of measurements of $2S_a/N$, from which we determine ζ_a^2. (**C**) Individual measurements of $2S_{n(\tau)}/N$ as a function of Rabi pulse length τ. The red line is a sinusoidal fit, from which we determine the Rabi contrast and $a \cdot n(\tau) = \cos[\vartheta(\tau)]$; see section 2 of (24). (**D**) Residuals of the fit in (C). (**E**) Measurement of $\mathcal{W}(\tau)$ as a function of $\vartheta(\tau)$. The red continuous line is the value of $\mathcal{W}(\tau)$ computed from the measurement of ζ_a^2 and the fitted Rabi oscillation [red line in (C)]. Bell correlations are present in the blue-shaded region. The observed four-fold symmetry of $\mathcal{W}(\tau)$ indicates that $a \cdot n(\tau)$ is well calibrated. The red square data point at $\vartheta = 128°$ violates the inequality in Eq. 3 by 3.8 standard deviations.

systems, especially of indistinguishable particles. Although this inequality was derived with assumptions about the measurement settings, it does not make any assumptions about the measured state. In particular, we do not need to assume that the state is symmetric under particle exchange. Moreover, this inequality applies whether the particles are spatially separated or not, similar to entanglement witnesses (22), under the common assumption that particles do not communicate (interact) through unknown channels. Although such an assumption would be questioned in a Bell test aimed at disproving the locally causal nature of the world, it is a well-satisfied and common assumption in the present context, where the goal is to explore correlations in a many-body system, assuming quantum mechanics to be valid.

For collective measurements, N is taken to be the number of detected particles, which may fluctuate slightly between experimental runs. If this is the case, we can replace N in Eq. 2 by the observable $\hat{N}$ and introduce the scaled collective spin $\mathcal{C}_n = \langle 2\hat{S}_n/\hat{N}\rangle$ and the scaled second moment $\zeta_a^2 = \langle 4\hat{S}_a^2/\hat{N}\rangle$; see section 1 of (24). The inequality then becomes

$$\mathcal{W} = -|\mathcal{C}_n| + (\boldsymbol{a} \cdot \boldsymbol{n})^2 \zeta_a^2 + 1 - (\boldsymbol{a} \cdot \boldsymbol{n})^2 \geq 0 \quad (3)$$

which is valid for any two axes $\boldsymbol{a}$ and $\boldsymbol{n}$ and for all non–Bell-correlated states. From this inequality, a criterion follows that will facilitate comparison with well-known spin-squeezing criteria: For any two axes $\boldsymbol{a}$ and $\boldsymbol{b}$ perpendicular to each other,

$$\zeta_a^2 \geq \frac{1}{2}\left(1 - \sqrt{1 - \mathcal{C}_b^2}\right) \quad (4)$$

holds for all non–Bell-correlated states [derivation in section 1.1 of (24)]. The experiment reported below shows a violation of the inequalities in Eqs. 3 and 4 in an atomic ensemble, hence demonstrating Bell correlations between the atomic spins.

We perform experiments with two-component Bose-Einstein condensates (BECs) of rubidium-87 atoms trapped magnetically on an atom chip (26) and prepared in a spin-squeezed state as in (18, 21) [see section 2 of (24)]. We start with a BEC without discernible thermal component in the ground-state hyperfine level $|F = 1, m_F = -1\rangle \equiv |1\rangle$. We are only concerned with the spin state of the atoms, whereas their uniform motional BEC state is irrelevant for the system's description. We perform only collective manipulations and measurements that are symmetric under particle exchange. A two-photon resonant Rabi field addresses the hyperfine transition from $|1\rangle$ to $|F = 2, m_F = 1\rangle \equiv |2\rangle$, with these two states representing a pseudospin 1/2 for each atom. The internal state of the entire BEC is described by a collective spin, with the component $\hat{S}_z = (\hat{N}_1 - \hat{N}_2)/2$ corresponding to half the atom number difference between the two states. With a $\pi/2$ Rabi pulse, we prepare a coherent spin state $[(|1\rangle + |2\rangle)/\sqrt{2}]^{\otimes N}$, in which the atomic spins are uncorrelated. To establish correlations between the spins, we make use of elastic

collisions, which give rise to a Hamiltonian $\hat{H} = \chi\hat{S}_z^2$. Controlling the rate χ with a state-dependent potential (21), we evolve the system in time with $\hat{H}$ to produce a spin-squeezed state (19, 27), which has reduced quantum noise in one collective spin component (Fig. 1A). To characterize this state, we count the numbers of atoms N_1 and N_2 in the two hyperfine states by resonant absorption imaging (21). We correct the data for imaging noise and collisional phase shifts. From averages over many measurements, we determine $\mathcal{C}_z$ and ζ_z^2. Projections along other spin directions are obtained by appropriate Rabi rotations before the measurement.

For the measurement of the Bell correlation witness $\mathcal{W}$, we use BECs with a total atom number of $N = 476 \pm 21$ (preparation noise after postselection) and $-5.5(6)$ dB of spin squeezing, according to the Wineland criterion (28). We first measure ζ_a^2, choosing $\boldsymbol{a}$ to be the squeezing axis where $\mathcal{C}_a \approx 0$ and ζ_a^2 is minimized (Fig. 1B). We find $\zeta_a^2 = 0.272(37)$; all quoted uncertainties are statistical standard deviations (SD). For the measurement of $\mathcal{C}_n$, we sweep the vector $\boldsymbol{n}$ in the plane defined by the state's center $\boldsymbol{b}$ and the vector $\boldsymbol{a}$ (Fig. 1A) by applying a Rabi pulse of duration τ. The measurement of $\mathcal{C}_{n(\tau)}$ as a function of τ is shown in Fig. 1C. From a sinusoidal fit to the observed Rabi oscillation, we obtain the Rabi contrast $\mathcal{C}_b = 0.980(2)$ as well as a precise calibration of $\boldsymbol{a} \cdot \boldsymbol{n}(\tau) = \cos[\vartheta(\tau)]$ needed to evaluate $\mathcal{W}$. From the resulting measurement of $\mathcal{W}(\tau)$ (Fig. 1E), we observe a violation of the inequality in Eq. 3 over a large range of angles. For $\vartheta = 128°$, we see the strongest violation with a statistical significance of 3.8 standard deviations (red square in Fig. 1E).

The inequality in Eq. 3 relies on a fine balance between competing terms, and a satisfactory demonstration of its violation depends on accurate knowledge of the angle ϑ between $\boldsymbol{a}$ and $\boldsymbol{n}$. The inequality in Eq. 4, on the other hand, is more robust to uncertainties in this angle and shows that our entire data set is inconsistent with the hypothesis of our state not being Bell-correlated. The black data point in Fig. 2 rep-

resents our data set by its Rabi contrast (the amplitude of the red fit in Fig. 1C) and squeezed second moment (Fig. 1B), giving an overall likelihood of 99.9% for Bell correlations [see section 2 of (24)]. This likelihood can be interpreted as a P value of 0.1% for excluding the hypothesis: Our data were generated by a state that has no Bell correlations, in the presence of Gaussian noise. An experiment closing the statistics loophole would exclude all possible non–Bell-correlated states, including those producing statistics with rare events. However, because of the way the bounds on $\mathcal{W}$ vary with N, such an experiment would require a number of measurements that increases with the number of spins [see section 3 of (24)].

We now discuss how our Bell correlation witness is connected to entanglement measures that were used previously to characterize spin-squeezed BECs (15, 19–22). These entanglement measures depend on the squeezed variance, for which the squeezed second moment ζ_a^2 is an upper bound (with equality if $\mathcal{C}_a = 0$, which is close to what we have measured). In terms of the latter, the Wineland spin-squeezing parameter (28) $\xi^2 \leq \zeta_a^2/\mathcal{C}_b^2$ witnesses entanglement (19) if $\xi^2 < 1$, shown as a red-shaded region in Fig. 2. Similarly, $(k+1)$–particle entanglement is witnessed by measuring squeezed variances (and hence ζ_a^2) below the gray k-producibility curves (20) in Fig. 2. These entanglement witnesses refer to the Ramsey contrast, whereas our data point in Fig. 2 refers to the measured Rabi contrast; in our experiment, these two quantities have nearly identical values. We can thus draw conclusions about both entanglement and Bell correlations from Fig. 2. In particular, we conclude that our witness requires at least 3 dB of spin squeezing for detecting Bell correlations.

We have shown that Bell correlations can be created and detected in many-body systems. This result has been obtained from a witness that requires collective measurements only. Although we have tested this witness with a spin-squeezed BEC, it could also be tested on other systems, such as thermal atoms in a spin-squeezed state.
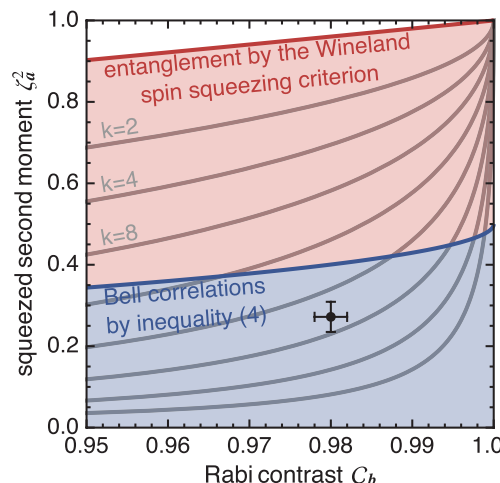
Fig. 2. Observation of Bell correlations in a BEC with the inequality in Eq. 4. The black circle shows the data set of Fig. 1 expressed in terms of the Rabi contrast $\mathcal{C}_b$ and the squeezed second moment ζ_a^2, with 1 SD error bars. The blue-shaded region shows Bell correlations detected by violation of the inequality in Eq. 4. A pair of random variables with the same parameters as our data set has a 99.9% overlap with this region [see section 2 of (24)]. The red-shaded region shows entanglement witnessed by spin squeezing (19, 28). The gray lines show limits on ζ_a^2 below which there is at least $(k+1)$–particle entanglement (20), increasing in powers of two up to $k = 256$. Our data set has a 99% overlap with the area below the limit for $k = 24$-particle entanglement.

Our results imply that the correlations between the atoms in a spin-squeezed Bose-Einstein condensate are strong enough to violate a Bell inequality. This Bell inequality could be violated directly by first localizing the atoms—e.g., through a nondestructive, spin-independent measurement of their position—and then measuring their internal states individually [see section 4 of (24)]. Further study of these states may enable insights into many-body correlations outside of the quantum formalism. Our results naturally raise the question of how our witness can be extended to detect genuine multipartite nonlocality (11) or to quantify the degree of nonlocality (29, 30), in a similar way as the degree of entanglement can be quantified in terms of k-producibility (Fig. 2) (20). Finally, Bell correlations are a resource in quantum information theory—e.g., for certifiable randomness generation. Although Bell-correlation–based randomness has been extracted from two-qubit systems (31), an implementation in a many-body system would considerably increase the amount of randomness per experimental run.

REFERENCES AND NOTES

1. N. Brunner, D. Cavalcanti, S. Pironio, V. Scarani, S. Wehner, *Rev. Mod. Phys.* **86**, 419–478 (2014).
2. J. S. Bell, *Between Science and Technology*, A. Sarlemijn, P. Kroes, Eds. (Elsevier, 1990), chap. 6.
3. V. Scarani, *Acta Physica Slovaca* **62**, 347–409 (2012).
4. B. P. Lanyon et al., *Phys. Rev. Lett.* **112**, 100403 (2014).
5. M. Eibl et al., *Phys. Rev. Lett.* **90**, 200403 (2003).
6. Z. Zhao et al., *Phys. Rev. Lett.* **91**, 180401 (2003).
7. J. Hofmann et al., *Science* **337**, 72–75 (2012).
8. W. Pfaff et al., *Nat. Phys.* **9**, 29–33 (2013).
9. M. Ansmann et al., *Nature* **461**, 504–506 (2009).
10. P. D. Drummond, *Phys. Rev. Lett.* **50**, 1407–1410 (1983).
11. G. Svetlichny, *Phys. Rev. D Part. Fields* **35**, 3066–3069 (1987).
12. M. Żukowski, Č. Brukner, *Phys. Rev. Lett.* **88**, 210401 (2002).
13. L. Amico, R. Fazio, A. Osterloh, V. Vedral, *Rev. Mod. Phys.* **80**, 517–576 (2008).
14. I. Bloch, J. Dalibard, W. Zwerger, *Rev. Mod. Phys.* **80**, 885–964 (2008).
15. C. Gross, T. Zibold, E. Nicklas, J. Estève, M. K. Oberthaler, *Nature* **464**, 1165–1169 (2010).
16. I. D. Leroux, M. H. Schleier-Smith, V. Vuletić, *Phys. Rev. Lett.* **104**, 250801 (2010).
17. A. Louchet-Chauvet et al., *New J. Phys.* **12**, 065032 (2010).
18. C. F. Ockeloen, R. Schmied, M. F. Riedel, P. Treutlein, *Phys. Rev. Lett.* **111**, 143001 (2013).
19. A. Sørensen, L.-M. Duan, J. I. Cirac, P. Zoller, *Nature* **409**, 63–66 (2001).
20. A. S. Sørensen, K. Mølmer, *Phys. Rev. Lett.* **86**, 4431–4434 (2001).
21. M. F. Riedel et al., *Nature* **464**, 1170–1173 (2010).
22. P. Hyllus, L. Pezzé, A. Smerzi, G. Tóth, *Phys. Rev. A* **86**, 012337 (2012).
23. J. Tura et al., *Science* **344**, 1256–1258 (2014).
24. Materials and methods are available as supplementary materials on *Science* Online.
25. J.-D. Bancal, N. Gisin, Y.-C. Liang, S. Pironio, *Phys. Rev. Lett.* **106**, 250404 (2011).
26. P. Böhi et al., *Nat. Phys.* **5**, 592–597 (2009).
27. M. Kitagawa, M. Ueda, *Phys. Rev. A* **47**, 5138–5143 (1993).
28. D. J. Wineland, J. J. Bollinger, W. M. Itano, D. J. Heinzen, *Phys. Rev. A* **50**, 67–88 (1994).
29. J.-D. Bancal, C. Branciard, N. Gisin, S. Pironio, *Phys. Rev. Lett.* **103**, 090503 (2009).
30. F. J. Curchod, N. Gisin, Y.-C. Liang, *Phys. Rev. A* **91**, 012121 (2015).
31. S. Pironio et al., *Nature* **464**, 1021–1024 (2010).
32. R. Schmied, P. Treutlein, *New J. Phys.* **13**, 065019 (2011).

GEOLOGY

Continental arc volcanism as the principal driver of icehouse-greenhouse variability

N. Ryan McKenzie,[1,2,3]* Brian K. Horton,[2,4] Shannon E. Loomis,[2] Daniel F. Stockli,[2] Noah J. Planavsky,[1] Cin-Ty A. Lee[5]

Variations in continental volcanic arc emissions have the potential to control atmospheric carbon dioxide (CO_2) levels and climate change on multimillion-year time scales. Here we present a compilation of ~120,000 detrital zircon uranium-lead (U-Pb) ages from global sedimentary deposits as a proxy to track the spatial distribution of continental magmatic arc systems from the Cryogenian period to the present. These data demonstrate a direct relationship between global arc activity and major climate shifts: Widespread continental arcs correspond with prominent early Paleozoic and Mesozoic greenhouse climates, whereas reduced continental arc activity corresponds with icehouse climates of the Cryogenian, Late Ordovician, late Paleozoic, and Cenozoic. This persistent coupled behavior provides evidence that continental volcanic outgassing drove long-term shifts in atmospheric CO_2 levels over the past ~720 million years.

Earth experienced multiple shifts in climate state over the past ~720 million years (My), with extensive icehouse intervals during the Cryogenian (1, 2), latest Ordovician (3), late Paleozoic (4), and mid-late Cenozoic alternating with greenhouse intervals during the early Paleozoic and Mesozoic–early Cenozoic eras (5, 6). These shifts are attributed to changes in the partial pressure of atmospheric carbon dioxide (Pco_2) (5–8). Long-term (≥10^6 years) changes in Pco_2 are controlled by the magnitude of carbon input to the ocean-atmosphere system from volcanic and metamorphic outgassing, as well as the removal of this carbon primarily through silicate weathering and subsequent precipitation and burial of carbonate minerals, along with organic carbon burial (8, 9). Although sporadic processes such as enhanced plume activity (10) and mountain building (11) have been invoked as drivers of specific greenhouse or icehouse intervals, no unifying model explains all of the observed fluctuations.

Arc magmatism along continental-margin subduction zones is thought to contribute more CO_2 to the atmosphere than other volcanic systems, owing to decarbonation of carbonates stored in the continental crust of the upper plate (12–16). Although direct measurements of CO_2 outgassing rates are limited, current continental volcanic arc (CVA) emissions are estimated to be as

[1]Department of Geology and Geophysics, Yale University, New Haven, CT 06511, USA. [2]Department of Geological Sciences, Jackson School of Geosciences, University of Texas at Austin, Austin, TX 78712, USA. [3]Department of Earth Sciences, University of Hong Kong, Pokfulam, Hong Kong, China. [4]Institute for Geophysics, Jackson School of Geosciences, University of Texas at Austin, Austin, TX 78712, USA. [5]Department of Earth Sciences, Rice University, Houston, TX 77005, USA.
*Corresponding author Email: ryan.mckenzie@yale.edu

Editor's Summary

Correlating an atomic condensate

Parts of a quantum system can be more "correlated" than what is allowed in the everyday classical world: A measurement on one part of the system can immediately affect a spatially distant component. The strongest of such correlations, Bell correlations, have been detected in small systems containing two to a handful of particles. Schmied *et al.* used collective measurements to detect Bell correlations among the spins of 480 Rb atoms cooled to a condensed state. This many-body correlated state may be useful as a resource in quantum information processing.

Science, this issue p. 441

Article Tools	Visit the online version of this article to access the personalization and article tools: http://science.sciencemag.org/content/352/6284/441
Permissions	Obtain information about reproducing this article: http://www.sciencemag.org/about/permissions.dtl